Role of Disulfide Bonds in the Structure and Potassium Channel Blocking Activity of ShK Toxin†

Michael W. Pennington,*,‡ Mark D. Lanigan,§ Katalin Kalman,|| Vladimir M. Mahnir,⊥ Heiko Rauer,|| Cheryl T. McVaugh,‡ David Behm,‡ Denise Donaldson,‡ K. George Chandy,|| William R. Kem,⊥ and Raymond S. Norton*,§

Bachem Bioscience Inc., 3700 Horizon Drive, King of Prussia, Pennsylvania 19406, Biomolecular Research Institute, 343 Royal Parade, Parkville 3052, Australia, Department of Pharmacology and Therapeutics, College of Medicine, University of Florida, Gainesville, Florida 32610-0267, and Department of Physiology and Biophysics, University of California, Irvine, California 92697

Received June 4, 1999; Revised Manuscript Received August 9, 1999

ABSTRACT: ShK toxin, a potassium channel blocker from the sea anemone *Stichodactyla helianthus*, is a 35 residue polypeptide cross-linked by three disulfide bridges: Cys3−Cys35, Cys12−Cys28, and Cys17−Cys32. To investigate the role of these disulfides in the structure and channel-blocking activity of ShK toxin, a series of analogues was synthesized by selective replacement of each pair of half-cystines with two α-amino-butyrate (Abu) residues. The remaining two disulfide pairs were formed unambiguously using an orthogonal protecting group strategy of Cys(Trt) or Cys(Acm) at the appropriate position. The peptides were tested in vitro for their ability to block Kv1.1 and Kv1.3 potassium channels and their ability to displace [^{125}I]dendrotoxin binding to rat brain synaptosomal membranes. The monocyclic peptides showed no activity in these assays. Of the dicyclic peptides, [Abu12,28]ShK$_{3-35,17-32}$ (where the subscript indicates disulfide connectivities) had weak activity on Kv1.3 and Kv1.1. [Abu17,32]ShK$_{3-35,12-28}$ blocked Kv1.3 with low nanomolar potency, but was less effective (being comparable to [Abu12,28]ShK$_{3-35,17-32}$) against Kv1.1. [Abu3,35]ShK$_{12-28,17-32}$, retained high picomolar affinity against both channels. Corroborating these results, [Abu3,35]ShK$_{12-28,17-32}$ had an IC$_{50}$ ratio relative to native toxin of 18 in the displacement assay, whereas [Abu17,32]ShK$_{3-35,12-28}$ and [Abu12,28]ShK$_{3-35,17-32}$ had ratios of 69 and 390, respectively. Thus, the disulfide bond linking the N- and C-terminal regions is less important for activity than the internal disulfides. NMR analysis of the [Abu12,28] and [Abu17,32] analogues indicated that they had little residual structure, consistent with their significantly reduced activities. By contrast, [Abu3,35]ShK$_{12-28,17-32}$ had a moderately well-defined solution structure, with a mean pairwise root-mean-square deviation of 1.33 Å over the backbone heavy atoms. This structure nevertheless showed significant differences from that of native ShK toxin. The possible interactions of this analogue with the channel and the distinction between native secondary and tertiary structure on one hand and global topology imposed by the disulfide bridges on the other are discussed.

Polypeptide toxins active against potassium channels have been isolated from the venoms of scorpions (*1*), snakes (*2*), cone snails (*3*), and sea anemones (*4*, *5*). ShK[1] toxin is a K^+ channel blocking polypeptide isolated from the sea anemone *Stichodactyla helianthus* (*4*) and subsequently synthesized (*6*). It is a 35 residue polypeptide stabilized by three intramolecular disulfide bonds (*7*). Although the molecule is of similar size and basicity to the scorpion toxins, its tertiary structure represents a novel fold dominated by two short α-helical stretches and several reverse turns, with a total absence of β-sheet (*8*), unlike the typical scorpion α/β fold (*9*).

Probing the K^+ channel-binding surface of ShK toxin shows that two residues, Lys22 and Tyr23, are crucial for activity (*10*−*12*). Studies on a related sea anemone toxin, BgK (*Bunodosoma granulifera*) toxin (*5*), have shown the same essential Lys-Tyr diad (*13*). This Lys-Tyr diad occurs in the second helix of the helix-kink-helix motif found in the anemone K^+ channel toxins (*8*, *13*). Intriguingly, the scorpion K^+ channel toxins utilize a similar binding motif, consisting of key Lys and aromatic (Tyr or Phe) residues on

† This work was supported in part by NIH Grant GM-54221 (W.R.K., R.S.N., M.W.P., and K.G.C.), Merck, Sharpe and Dohme (K.G.C.), and the Alexander von Humboldt foundation (H.R.).

* To whom correspondence should be addressed. (M.W.P.) Fax: +1-610-239-0800. E-mail: mpennipep@aol.com. (R.S.N.) Fax: +61-3-9903 9655. E-mail: ray.norton@bioresi.com.au.

‡ Bachem Bioscience Inc..

§ Biomolecular Research Institute.

|| University of California, Irvine.

⊥ University of Florida College of Medicine.

[1] Abbreviations: AcOH, acetic acid; Acm, acetamidomethyl; Boc, *tert*-butyloxycarbonyl; DTX, dendrotoxin I from *Dendroaspis polylepis*; Fmoc, 9-fluorenylmethyloxycarbonyl; NOE, nuclear Overhauser enhancement; NOESY, 2D nuclear Overhauser enhancement spectroscopy; Pmc, 2,2,5,7,8-pentamethylchroman-6-sulfonyl; RMSD, root-mean-square deviation; RP-HPLC, reversed-phase high-performance liquid chromatography; ShK toxin, *Stichodactyla helianthus* potassium channel blocking toxin; tBu, tbutyl; TFA, trifluoroacetic acid; Trt, triphenylmethyl.

10.1021/bi991282m CCC: $18.00
Published on Web 10/14/1999

the binding surface (*14*−*16*). In addition to Lys22 and Tyr23, other residues also contribute to the K^+ channel-binding surface of ShK toxin. Arg11 was important for activity against Jurkat T-lymphocytes but not for rat brain binding (*10*), while an alanine scan showed that Ile7, Ser20, and Phe27 also contributed to rat brain binding (*11*). More recently, functional assays on the Kv1.3 K^+ channel subtype expressed in mammalian cells identified His19, Ser20, and Arg24 as important (*17*), although the role of His19 may be at least partly structural (*18*) and its significance was inferred using an H19K mutant rather than H19A, as the latter did not fold in reasonable yield (*11*).

In this study, we have investigated the importance of the structure-stabilizing elements in ShK toxin. These are dominated by the three intramolecular disulfide bonds, with a lesser contribution from a salt bridge between Asp5 and Lys30 (*8*, *10*, *11*, *18*). In an earlier report, we showed that truncation of the N- and C-termini, thereby eliminating the Cys3−Cys35 disulfide bond, reduced activity to less than 0.1% of wild-type toxin (*19*). A series of peptides containing two of the three natural disulfide bonds has now been prepared, where the two Cys residues comprising the third disulfide have been replaced with the neutral isostere α-amino butyrate, viz., [Abu3,35]$ShK_{12-28,17-32}$ (where the pairings of the remaining disulfides are indicated by subscript), [Abu12,28]$ShK_{3-35,17-32}$, or [Abu17,32]$ShK_{3-35,12-28}$. Since native ShK toxin inhibits the cloned Kv1.1, Kv1.3, Kv1.4, and Kv1.6 channels at picomolar concentrations, and the Kv1.2, Kv1.7, and IKCa1 channels at nanomolar concentrations (*20*), we performed two assays to test whether the synthetic peptides retained their potency for the target channels. In the first assay, the analogues were tested for their potency in blocking K^+ currents through cloned Kv1.1 and Kv1.3 channels expressed in *Xenopus* oocytes and in mammalian cells. The most potent analogue, [Abu3,35]$ShK_{12-28,17-32}$, was also tested on Kv1.2, Kv1.7, and IKCa1 channels. In the second, we examined the ability of the analogues to compete with the binding of radioiodinated dendrotoxin to K^+ channels in rat brain membranes that are composed primarily of heteromultimers of Kv1.1 and Kv1.2 subunits. Each polypeptide was also investigated by 2D NMR to assess the effect of disulfide bond replacement on the structure of the toxin. Although two of the analogues had little residual structure, the third had a moderately well-defined solution structure that was determined using NMR data and compared with that of native ShK toxin. The structural changes caused by loss of the 3−35 disulfide are discussed in relation to the reduced K^+ channel blocking activity of this analogue.

MATERIALS AND METHODS

Natural Toxins. Dendrotoxin I (DTX), isolated from *Dendroaspis polylepis*, was graciously provided by Dr. E. Karlsson, Biomedical Center, University of Uppsala, Uppsala, Sweden. Wild-type ShK toxin and radioiodinated dendrotoxin I were prepared according to previously described methods (*6*). All other reagents were of the finest grade commercially available.

Synthesis of ShK Toxin Analogues. Fmoc-amino acids were obtained from Bachem AG (Bubendorf, Switzerland). Stepwise assembly was carried out starting with either 0.125 mmol of Fmoc-Cys(Trt)-2-chlorotrityl-resin (0.65 mmol/g) or Fmoc-α-Abu-Wang resin on an Applied Biosystems 431A peptide synthesizer at the 0.25 mmol scale, and the remaining amino acid sequence incorporating the substitution was assembled as described previously (*10*, *11*). Disulfides were replaced by substituting α-Abu for the two half-cystines. The remaining four Cys residues required orthogonal protecting groups for correct placement of the two disulfide bonds. For [Abu12,28]$ShK_{3-35,17-32}$ toxin, these were Cys(Trt) at Cys3 and Cys35, and Cys(Acm) for Cys17 and Cys32. For the other analogues, the following strategies were employed. [Abu3,35]$ShK_{12-28,17-32}$ toxin, Fmoc-α-Abu-Wang resin, Cys12-Cys28: Cys(Trt) and Cys17-Cys32: Cys(Acm). [Abu17,32]$ShK_{3-35,12-28}$ toxin, Fmoc-Cys(Trt)-2-chlorotrityl resin, Cys3-Cys35: Cys(Trt). Cys12-Cys28: Cys(Acm). Ala was substituted for Met21 in all three analogues. Following removal of the Fmoc group, each peptide was cleaved with reagent K (*21*) for 2 h at room temperature. The free peptide was then filtered to remove spent resin beads, precipitated with ice-cold diethyl ether, collected on a fine filter by suction, washed with ice-cold ether, and finally extracted with 20% AcOH in H_2O.

Oxidative formation of the first disulfide bond of each analogue was accomplished by diluting the crude peptide solution into water to a concentration of 0.1 mg/mL. The pH of the solution was adjusted to 8.0 with ammonium hydroxide, and the peptide allowed to oxidize in the presence of air until Ellman's test (*22*) was negative (usually within 24 h). The monocyclic products were purified by RP-HPLC using a TFA-buffered aqueous acetonitrile gradient. HPLC-pure fractions were pooled and lyophilized. The monocyclic product was converted directly to the dicyclic product by oxidative cleavage of the Cys(Acm) protecting groups with I_2, according to the procedure of Veber et al. (*23*). The dicyclic products were purified by RP-HPLC as described above. Structures and the purity of all analogues were assessed by HPLC, circular dichroism spectroscopy (*24*), and amino acid and ESI-MS analysis.

The truncated analogues [Nle21]$ShK(9-32)_{12-28,17-32}$ and [Cys(Acm)12,28, Nle21]$ShK(9-32)_{17-32}$ were prepared as described previously (*19*).

NMR Spectroscopy. Two-dimensional ^1H NMR spectra were recorded at either 500 or 600 MHz on a 5.6 mM solution of [Abu3,35]$ShK_{12-28,17-32}$ (pH 5.0) and 2.5 mM solutions of [Abu12,28]$ShK_{3-35,17-32}$ and [Abu17,32]$ShK_{3-35,12-28}$ (pH 4.9) in 90% H_2O/10% ^2H_2O (v/v) at 293 K. All 2D spectra were recorded essentially as described previously (*8*, *25*), but with water suppression by means of pulsed field gradients using the WATERGATE scheme and a 3-9-19 selective pulse (*26*).

Structure Calculations. Methods for obtaining distance and angle restraints and generating structures in DYANA (*27*) were similar to those described previously (*8*, *25*) except that distances for initial structures were calculated using volumes proportional to r^{-4}. The final set of restraints were calculated using volumes proportional to r^{-6}, following which a new family of structures was generated using DYANA. The 50 DYANA structures with the lowest penalty functions were refined by restrained simulated annealing and restrained energy minimization in X-PLOR (*28*) as described previously (*8*, *25*). The final NMR restraint list (from which values redundant with the covalent geometry had been eliminated by DYANA) consisted of 136 intraresidue, 95 sequential,

78 medium-range ($|i - j| < 5$) and 19 long-range ($|i - j| \geq 5$) upper bound restraints, 3 lower bound restraints, and 26 backbone dihedral angle restraints. Of the 50 CHARMM-minimized structures, the best 25 were chosen on the basis of their stereochemical energies. Of these, the best 20 were chosen on the basis of the consistency of their secondary structures with the NMR restraints. These structures and the NMR restraints on which they were based have been submitted to the Protein Data Bank (*29*) (accession code 1C2U).

Structures were analyzed using Insight II (Molecular Simulations Inc, San Diego), PROCHECK_NMR (*30*) and MOLMOL 2.6 (*31*). Hydrogen bonds were identified in MOLMOL using a maximum C−N distance of 2.7 Å and a maximum angular deviation of 60° from linearity.

Electrophysiological Assays. The expression constructs encoding Kv1.1, Kv1.2, Kv1.3, and the two Kv1.3 mutants (H404V and D386N) have been described previously (*16*, *32*). The cRNA was transcribed in vitro and injected into oocytes (*Xenopus laevis*, from NASCO, Fort Atkinson, WI) (*20*). Potassium currents were measured at room temperature using the two-voltage clamp technique (*20*), and data were analyzed using pClamp software (version 5.5.1, Axon instruments, Burlingame, CA). Whole oocytes were held at −100 mV and depolarized to +40 mV over 500 ms; time between pulses was 30 s. Capacitative and leak currents were subtracted prior to analysis using the P/4 procedure. The dissociation constant was calculated assuming a 1:1 binding of toxin to channel as described previously (*20*).

The Kv1.3 and IKCa1 constructs were also expressed in mammalian cells. The human IKCa1 construct was linearized with *Not*I and transcribed in vitro (*16*, *33*). The cRNA along with a marker dye was injected into rat basophilic leukemia cells as described previously (*20*, *33*, *34*). After 2−6 h, visualized cells with specific currents could be characterized using the patch-clamp method. Cells stably expressing Kv1.3 (*32*) were trypsinized and plated onto glass cover slips at least 3 h prior to measurement. All cells were measured in the whole-cell configuration and bathed in mammalian Ringer solution with 0.1% bovine serum albumin (Sigma, St. Louis, MO) containing (mM): 160 NaCl, 4.5 KCl, 2 $CaCl_2$, 1 $MgCl_2$, and 10 Hepes adjusted to pH 7.4 with NaOH, with an osmolarity of 290−320 mOsm. A simple syringe-driven perfusion system was used to exchange the bath solutions in the recording chamber. The internal pipet solution for the Kv1.3 channel recordings contained (mM): 134 KF, 1 $CaCl_2$, 2 $MgCl_2$, 10 Hepes, 10 EGTA, pH 7.2 (with KOH), and 290−310 mOsm. The internal pipet solution for the IKCa1 channel contained (mM): 135 potassium-aspartate, 2 $MgCl_2$, 10 Hepes, 10 EGTA, 8.7 $CaCl_2$, pH 7.2 (with KOH), and 290−310 mOsm ($[Ca^{2+}{}_i]_{free} = 10^{-6}$ M). The holding potential in all experiments was −80 mV. IKCa1 currents were elicited by activation with 1 μM internal Ca^{2+} and voltage ramps from −150 to 50 mV applied every 5 s and lasting 200 ms. Kv1.3 currents were measured following depolarizing pulses (200 ms in duration) to 40 mV from the holding potential, applied every 30 s. Series resistance compensation (80%) was used if the current exceeded 2 nA. Capacitative and leak currents were subtracted using the P/10 procedure for Kv1.3 currents. K_d values were calculated using the equation $K_d = ([\text{toxin}]/[(1/y) - 1)]$ (mean ± SD, $n \geq 3$, for all experiments).

Binding Assays. The procedures for measuring displacement of [^{125}I]DTX binding to rat brain membranes were described previously (*6*). In brief, ShK toxin and its analogues were incubated with rat brain membranes (0.2 mg of protein) and 1 nM [^{125}I]DTX (34 Ci/mmol) for 1 h at room temperature, in a buffer containing 150 mM NaCl, 30 mM Tris-HCl, and 1 mg/mL BSA, pH 7.0, with total volume 0.25 mL. Nonspecific binding was measured with 1 μM cold DTX. The measurements were performed in triplicate; the standard errors of mean measurements were generally less than 6%.

Because of the relatively low specific radioactivity of the [^{125}I]DTX and a relatively high nonspecific binding (35−40% of total bound toxin) caused by the presoaked glass filters, a relatively high concentration of membrane protein was used in the binding assays. Thus, the free [^{125}I]DTX in each membrane-containing tube was probably much less than the total [^{125}I]DTX added initially. Since our IC_{50} values were estimated using total initial concentrations of ShK toxin, rather than their steady-state free concentrations, they probably underestimate the true affinities of the toxins for the K^+ channels. However, this would not affect the IC_{50} ratios considered below, because identical conditions were used for measurements of both the wild-type toxin and each ShK analogue. The binding interaction between dendrotoxins and either charybdotoxin (*35*) or ShK (Mahnir et al., unpublished results) is best characterized as a noncompetitive interaction, so this also prevents calculation of K_d values for ShK inhibition of DTX binding by the Cheng-Prusoff equation. Using Scatchard analysis of [^{125}I]DTX binding to the rat membranes, we observed a concentration of DTX-binding sites (650 fmol/mg membrane protein), very similar to the estimated concentration of charybdotoxin binding sites in rat brain (*35*).

RESULTS

Peptide Synthesis and Characterization. The primary structures of ShK toxin and its analogues are given in Figure 1. The peptides were synthesized on either 0.125 mmol of Fmoc-Cys(Trt)-2-chlorotrityl resin or Fmoc-α-Abu-Wang resin. For the peptides containing a C-terminal Cys, 2-chlorotrityl resin was employed to help suppress racemization of the C-terminal Cys residue (*36*). In each peptide, one pair of Cys residues was replaced with α-Abu as an isosteric replacement. Additionally, one of the Cys pairs was substituted with Cys protected on the thiol function with an acetamidomethyl group and the second pair protected with trityl, allowing specific placement of both disulfide bonds. To prevent oxidative side reactions, Met21 was substituted with Ala, as previous studies had shown that Ala substitution for Met21 had little effect on toxin activity (*11*). These side reactions occurred in an initial synthesis of one of the peptides following treatment with I_2 to cleave the Acm-protecting groups and form the second disulfide bridge. Following chain assembly and acidolytic cleavage, the crude reduced peptides were cyclized, yielding the monocyclic (one disulfide bond) products at the two Cys residues that had been protected with Trt. Yields for each of the monocyclic products were between 30 and 45% of theory. Samples of each of the monocyclic products were retained for bioassay, and the remainder converted directly to the dicyclic product by treatment with I_2. Conversion to the dicyclic form was

	5 10 15 20 25 30 35
$ShK_{3-35,12-28,17-32}$ (WT)	RS**C**IDTIPKSR**C**TAFQ**C**KHSMKYRLSF**C**RKT**C**GT**C**
[Abu3,35]$ShK_{12-28,17-32}$	RS**B**IDTIPKSR**C**TAFQ**C**KHSAKYRLSF**C**RKT**C**GT**B**
[Abu3,35]ShK_{12-28}	RS**B**IDTIPKSR**C**TAFQ***c***KHSAKYRLSF**C**RKT***c***GT**B**
[Abu12,28]$ShK_{3-35,17-32}$	RS**C**IDTIPKSR**B**TAFQ**C**KHSAKYRLSF**B**RKT**C**GT**C**
[Abu12,28]ShK_{3-35}	RS**C**IDTIPKSR**B**TAFQ***c***KHSAKYRLSF**B**RKT***c***GT**C**
[Abu17,32]$ShK_{3-35,12-28}$	RS**C**IDTIPKSR**C**TAFQ**B**KHSAKYRLSF**C**RKT**B**GT**C**
[Abu17,32]ShK_{3-35}	RS**C**IDTIPKSR***c***TAFQ**B**KHSAKYRLSF***c***RKT**B**GT**C**
$ShK(9-32)_{12-28,17-32}$	KSR**C**TAFQ**C**KHS***n***KYRLSF**C**RKT**C**
$ShK(9-32)_{17-32}$	KSR***c***TAFQ**C**KHS***n***KYRLSF***c***RKT**C**

FIGURE 1: Primary structures (one letter code) of ShK toxin and its analogues lacking one or more disulfide bridges. The sequence of wild-type ShK is shown with its disulfide connectivities as lines. The position of the half-cystines are indicated, as are Abu (B), Nle (*n*), and Cys-Acm (*c*). The nomenclature of each analogue is such that the location of Abu substitutions are indicated within each bracket and the remaining disulfide pairings are in subscript.

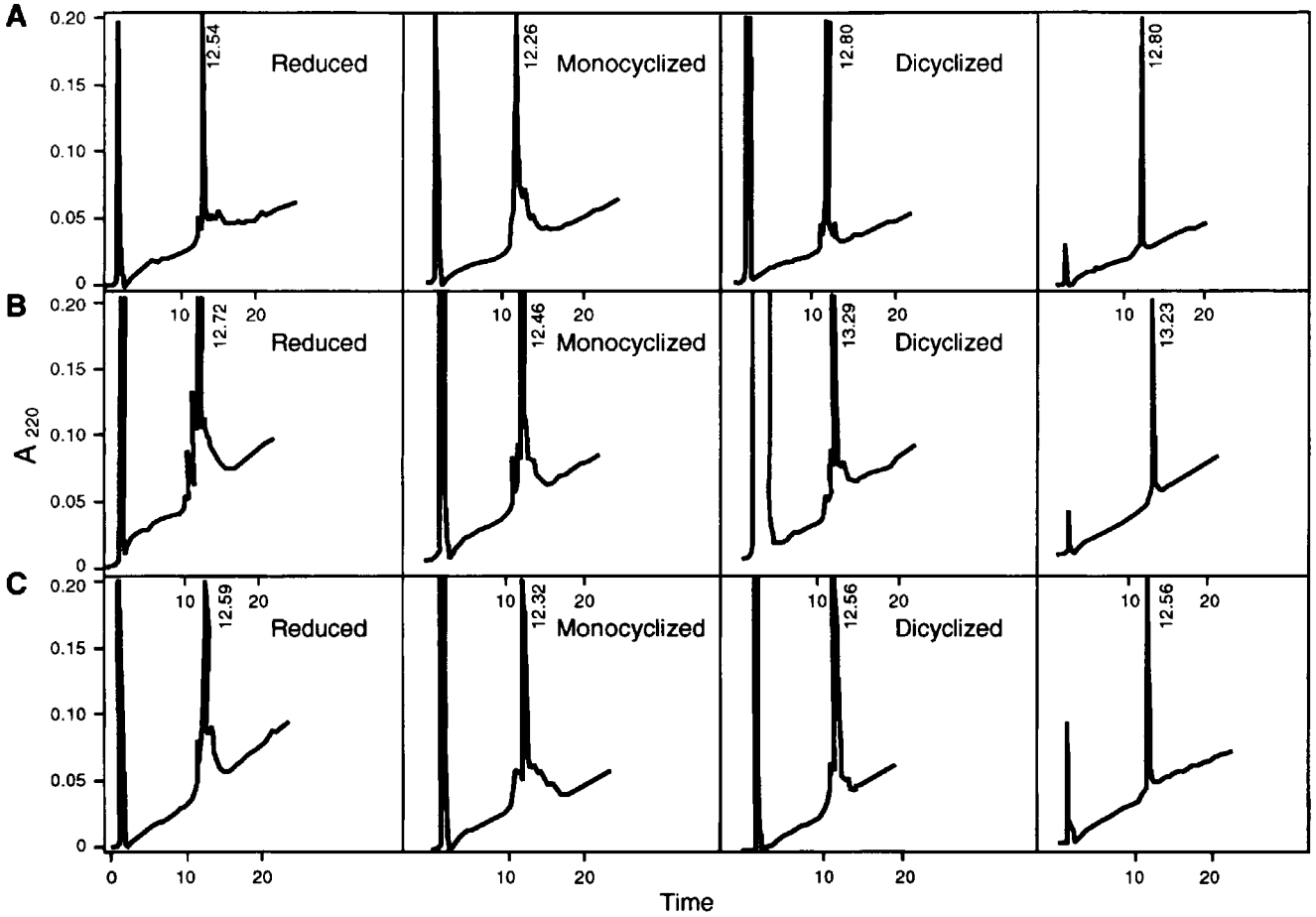

FIGURE 2: Analytical RP-HPLC profiles of (A) [Abu3,35]$ShK_{12-28,17-32}$, (B) [Abu12,28]$ShK_{3-35,17-32}$, and (C) [Abu17,32]$ShK_{3-35,12-28}$ at different levels of cyclization. The crude reduced peptides after TFA cleavage (left panel), after formation of the first disulfide bond via air oxidation (second panel from left), after formation of the second disulfide bond (dicylized) via treatment with I_2 (third panel from the left) and final purified dicyclized product (right panel) are shown.

followed by analytical HPLC and was complete within 1 h. Each of the dicyclic peptides shifted to a later retention time following cleavage of the polar Acm protecting groups, as shown in Figure 2. Electrospray mass spectrometry of the oxidized monocyclic (diAcm) and dicyclic peptides gave experimental M_r values of 4102.9 (expected 4103.4) and 3959.6 (expected 3960.3), respectively.

Effect of ShK Analogues on cloned Kv Channels. The cloned K^+ channels, Kv1.1, Kv1.3, Kv1.4, and Kv1.6, are blocked by ShK toxin with K_d in the low picomolar range, while the related Kv1.2 and Kv1.7 channels and the intermediate-conductance calcium-activated K^+ channel, IKCa1, are blocked at nanomolar concentrations (*17*, *20*). In contrast, cloned Kv1.5, Kv3.1, and Kv3.4 channels are all resistant

Table 1: Effect of ShK Analogues on Kv1.1 and Kv1.3 Channels Expressed in *Xenopus* Oocytes

	Kv1.1		Kv1.3	
ShK analog	K_d (pM)	K_d analog/K_d ShK	K_d (pM)	K_d analog/K_d ShK
ShK	6.7 ± 3		4.7 ± 0.9	
[Abu12,28]$ShK_{3-35,17-32}$	23 450 ± 1680	3500	94 800 ± 9430	20 170
[Abu17,32]$ShK_{3-35,12-28}$	51 460 ± 5220	7680	2644 ± 491	563
[Abu3,35]$ShK_{12-28,17-32}$	1045 ± 498	156	462 ± 9	98
[Abu12,28]ShK_{3-35}	>100 000		>715 000	
[Abu17,32]ShK_{3-35}	>500 000		>900 000	
[Abu3,35]ShK_{12-28}	>500 000		>316 000	

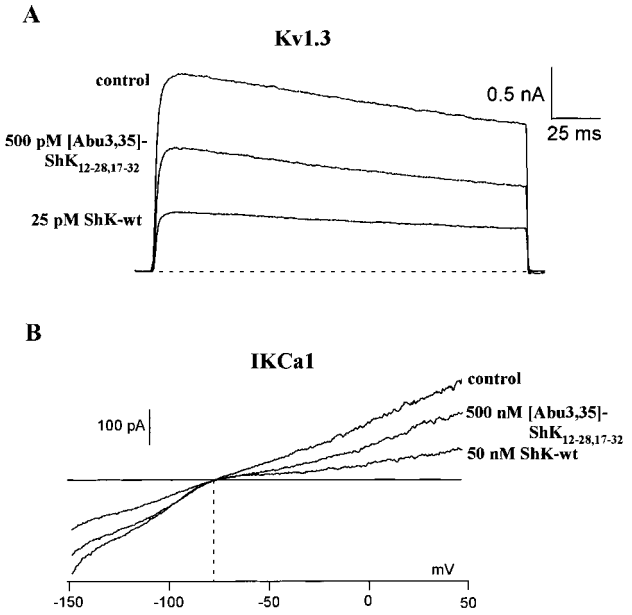

FIGURE 3: Effect of ShK and [Abu 3,35]$ShK_{12-28,17-32}$ on Kv1.3 and IKCa1 currents exogeneously expressed in rat basophilic leukemia cells. (A) Wild-type ShK and [Abu 3,35]$ShK_{12-28,17-32}$ block currents through Kv1.3 at low and high picomolar concentrations, respectively. The K_d for ShK is 16 ± 3 pM (n = 6) and for [Abu 3,35]$ShK_{12-28,17-32}$ 762 ± 88 pM (n = 4). (B) Currents through IKCa1 are blocked at low and high nanomolar concentrations of wild-type ShK and [Abu 3,35]$ShK_{12-28,17-32}$, respectively. The K_d for ShK is 30 ± 7 nM (n = 8) and for [Abu 3,35]$ShK_{12-28,17-32}$ 981 ± 189 nM (n = 3).

to this toxin (*20*). To determine whether the ShK analogues with modified disulfide bridges were functional, we examined their ability to block Kv1.1 and Kv1.3 channels expressed in *Xenopus* oocytes. When applied externally, each of the monocyclic peptides was devoid of activity on both channels (Table 1). The three dicyclic analogues varied in their ability to block Kv1.1 and Kv1.3. [Abu12,28]$ShK_{3-35,17-32}$ showed weak activity against both channels, indicating that the internal Cys12−Cys28 disulfide is critical for maintaining a structure that retains binding to these K^+ channels. [Abu17,32]$ShK_{3-35,12-28}$ exhibited low nanomolar potency against Kv1.3, but was significantly less effective against Kv1.1. [Abu3,35]$ShK_{12-28,17-32}$ retained high picomolar affinity against Kv1.3 and blocked Kv1.1 at low nanomolar concentrations.

The ability of [Abu3,35]$ShK_{12-28,17-32}$ to inhibit IKCa1, Kv1.2, and Kv1.7 channels was also tested. Figure 3 compares the effect of ShK toxin and [Abu3,35]$ShK_{12-28,17-32}$ on Kv1.3 and IKCa1 channels expressed in mammalian cells. ShK, when applied externally, blocked the Kv1.3 and IKCa1 channels with K_d values of 16 ± 3 pM and 30 ± 7 nM, respectively. Consistent with the oocyte data, replacement of the Cys3−Cys35 bond resulted in only a modest reduction in activity (Kv1.3 K_d = 762 ± 88 pM; IKCa1 K_d = 981 ± 189 nM). In separate experiments, [Abu3,35]$ShK_{12-28,17-32}$ was found to retain nanomolar affinity for the Kv1.2 channel (K_d = 56 ± 10 nM; ShK K_d = 9 ± 3 nM) but was relatively inactive against Kv1.7 (K_d >1 μM; ShK K_d = 11.5 ± 2.3 nM). These data indicate that the internal disulfide bonds at Cys12−Cys28 and Cys17−Cys32 are more important for maintaining a structure that retains K^+ channel binding than the more solvent-exposed Cys3−Cys35 disulfide. Moreover, perturbations of the structure in the three dicyclic analogues differentially affect the toxin's ability to block the five K^+ channels tested.

Table 2: Displacement of [^{125}I]DTX from Rat Brain Synaptosomal Membranes by ShK Toxin Analogues

ShK analog	IC_{50} (nM)	IC_{50} analog/IC_{50} ShK
ShK	5.37 ± 0.46[a]	
[Abu12,28]$ShK_{3-35,17-32}$	2107 ± 394	390
[Abu17,32]$ShK_{3-35,12-28}$	370 ± 12	69
[Abu3,35]$ShK_{12-28,17-32}$	96.8 ± 0.3	18
[Abu12,28]ShK_{3-35}	>8000	>2850[b]
[Abu17,32]ShK_{3-35}	>8000	>2850[b]
[Abu3,35]ShK_{12-28}	>8000	>2850[b]

[a] One standard error is shown on these IC_{50} values [b] The IC50 for ShK displacement of [^{125}I]DTX in this series of experiments was 2.8 ± 0.3 nM.

Binding Affinity. DTX-sensitive potassium channels in the brain are largely heteromultimers composed of Kv1.1 and Kv1.2, as well as other subunits (*37*). It has been reported that about 30% of the rat brain potassium channels that bind the scorpion toxin hongotoxin are composed only of Kv1.1 and Kv1.2 subunits, while others containing Kv1.3, Kv1.4, and/or Kv1.6 subunits in addition to Kv1.1 and Kv1.2 (*38*) constitute the remaining channel sub-populations. Native ShK inhibits [^{125}I]DTX binding to K^+ channels in rat brain synaptosomes at low nanomolar concentrations (Table 2), presumably by interacting with these heteromultimeric channels (*20*). Despite the channel heterogeneity, ShK inhibits DTX binding as if there were a single population of DTX-binding sites (*6*). Table 2 compares the IC_{50} values for each of the analogues with that of native ShK in competition experiments with [^{125}I]DTX for binding to rat brain synaptosomal membranes. Consistent with the electrophysiological data, each of the monocyclic peptides was essentially devoid of binding affinity, while the dicyclic products showed a similar potency profile as for block of the cloned channels, [Abu 3,35]$ShK_{12-28,17-32}$ exhibiting only a modest reduction in affinity.

Since homotetrameric Kv1.2 channels are 1000-fold less sensitive to ShK relative to Kv1.1, Kv1.4, and Kv1.6 homotetramers (*20*), the presence of one or more Kv1.2

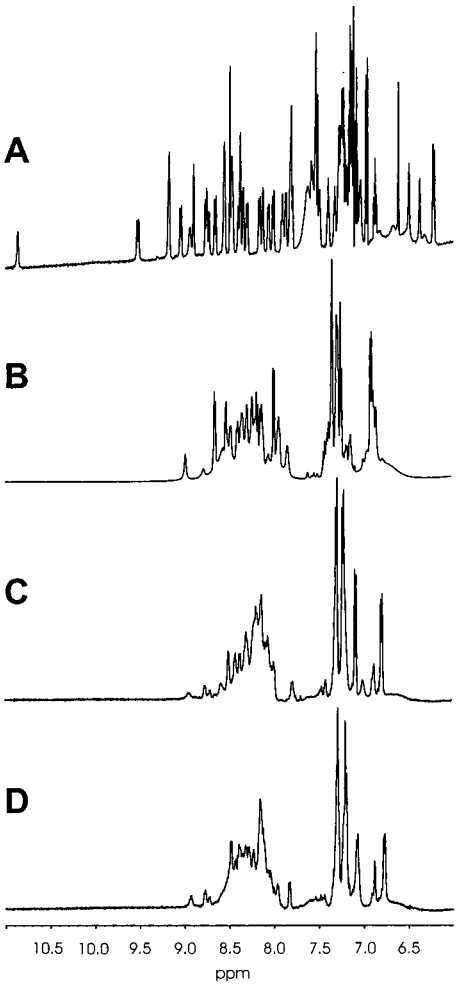

FIGURE 4: Amide and aromatic regions of 500 MHz ^{1}H NMR spectra of (A) ShK (wild-type), (B) [Abu3,35]ShK$_{12-28,17-32}$, (C) [Abu12,28]ShK$_{3-35,17-32}$, and (D) [Abu17,32]ShK$_{3-35,12-28}$ at 293 K.

subunits in the majority of rat brain Kv1 channels may be partly responsible for the significantly lower affinity of ShK for rat brain synaptosomes (Table 2). To test this idea, we measured the potency of native ShK and [Abu3,35]-ShK$_{12-28,17-32}$ on Kv1.1-Kv1.2 heteromultimers expressed in *Xenopus* oocytes. A dimeric construct containing one Kv1.1 subunit and one Kv1.2 subunit was used for these experiments, the functional tetramer most likely being composed of two Kv1.1 and two Kv1.2 subunits**.** The K_d values for ShK and [Abu3,35]ShK$_{12-28,17-32}$ were 1.4 and 24.2 nM, respectively, in good agreement with the rat brain binding data (Table 2).

NMR Analyses. To assess the conformational sequelae of the various disulfide bond replacements, each of the peptides was analyzed by ^{1}H NMR spectroscopy. Figure 4 shows the amide and aromatic regions of 1D ^{1}H NMR spectra of native ShK and the three diAbu-substituted analogues. The spectral dispersion apparent in native ShK (Figure 4A) is diminished considerably in the three Abu analogues (Figure 4, panels B−D). Because of pronounced peak overlap in spectra of these analogues, sequential resonance assignments were obtained only for [Abu3,35]ShK$_{12-28,17-32}$. A table of chemical shifts for this analogue is included in the Supporting Information, together with figures summarizing the sequential assignments, backbone coupling constants, and medium-range NOEs and the chemical shift deviations from random-coil values (*39*). This lack of spectral dispersion suggests some disruption of the conformations of the analogues compared with that of native ShK. Indeed, the NN regions of NOESY spectra of [Abu12,28]ShK$_{3-35,17-32}$ and [Abu17,32]ShK$_{3-35,12-28}$ (Figure 5) lack a considerable number of d_{NN} connectivities that are present in the spectrum of native ShK toxin and are characteristic of its helical structure. By contrast, [Abu3,35]ShK$_{12-28,17-32}$, despite the reduction in its spectral dispersion compared with ShK, shows a number of d_{NN} connectivities (Figure 5B), albeit not as many as in the native toxin.

The profiles of differences from random-coil chemical shifts for ShK and [Abu3,35]ShK$_{12-28,17-32}$ are similar over residues 14−24, with negative C$^\alpha$H differences in this region suggesting the presence of α-helix, as in ShK itself. This implies that [Abu3,35]ShK$_{12-28,17-32}$ has retained some native-like structure, although the N- and C-termini may adopt nonnative-like conformations.

Structure of [Abu3,35]ShK$_{12-28,17-32}$. The solution structure of [Abu3,35]ShK$_{12-28,17-32}$ was determined using distance and angle restraints obtained from NOESY and DQF-COSY spectra at 293 K. The structural statistics for [Abu3,35]ShK$_{12-28,17-32}$ (Table 3) show that the structures are in good agreement with the experimental restraints and have good stereochemistry. Moreover, 98% of the residues have $\phi-\psi$ values in the generously allowed regions of a Ramachandran plot (*30*). The angular order parameters (S) of the final 20 structures indicate that residues 4, 8−31, 34, and 35 are well-defined locally, with $S > 0.8$ for both ϕ and ψ angles (Figure 6, panels C and D). The backbone RMSD from the mean structure (Figure 6B) also shows that the structure is well-defined over most of the molecule. The higher RMSD values near the N-terminus reflect the paucity of NOEs defining that region (Figure 6A).

Figure 7A shows the family of 20 lowest-energy NMR-derived structures of [Abu3,35]ShK$_{12-28,17-32}$. The main secondary structure elements as determined by MOLMOL are one turn of 3_{10}-helix between residues 19−21 (in 75% of the structures) and α-helix between residues 22−25. Although the latter helix is present in only 35% of the structures, there are two backbone hydrogen bonds in this region, 24 → 21 and 25 → 21, in all structures. Similarly, the 3_{10}-helix includes three backbone hydrogen bonds, 21 → 18 (60% of structures), 21 → 19 (95% of structures), and 22 → 19 (95% of structures). There are a number of $d_{\alpha\beta}$-(i,i+3) connectivities observed in [Abu3,35]ShK$_{12-28,17-32}$ between residues 14−24. While these suggest the presence of α-helix in this region, the medium-range NOEs [$d_{\alpha N}$(i,i+3) and $d_{\alpha N}$(i,i+4)] and low $^3J_{HNH\alpha}$ coupling constants characteristic of this structure are not observed.

Comparison with ShK. Native ShK toxin (*8*) contains two short α-helices between residues 14−24, with a bend at Ser20, and adopts a fairly compact structure. By contrast, in [Abu3,35]ShK$_{12-28,17-32}$, the helices are poorly defined and the conformations of the N- and C-terminal regions are altered as a result of the absence of the 3−35 disulfide bridge, as shown in Figure 7. Pairwise RMS differences over the backbone heavy atoms (N, C$^\alpha$, and C) between the closest-to-average structures for ShK and the analogue are 8.29 Å over residues 1−35 and 5.96 Å over residues 9−31. Considering the α-helical region of ShK (residues 14−24),

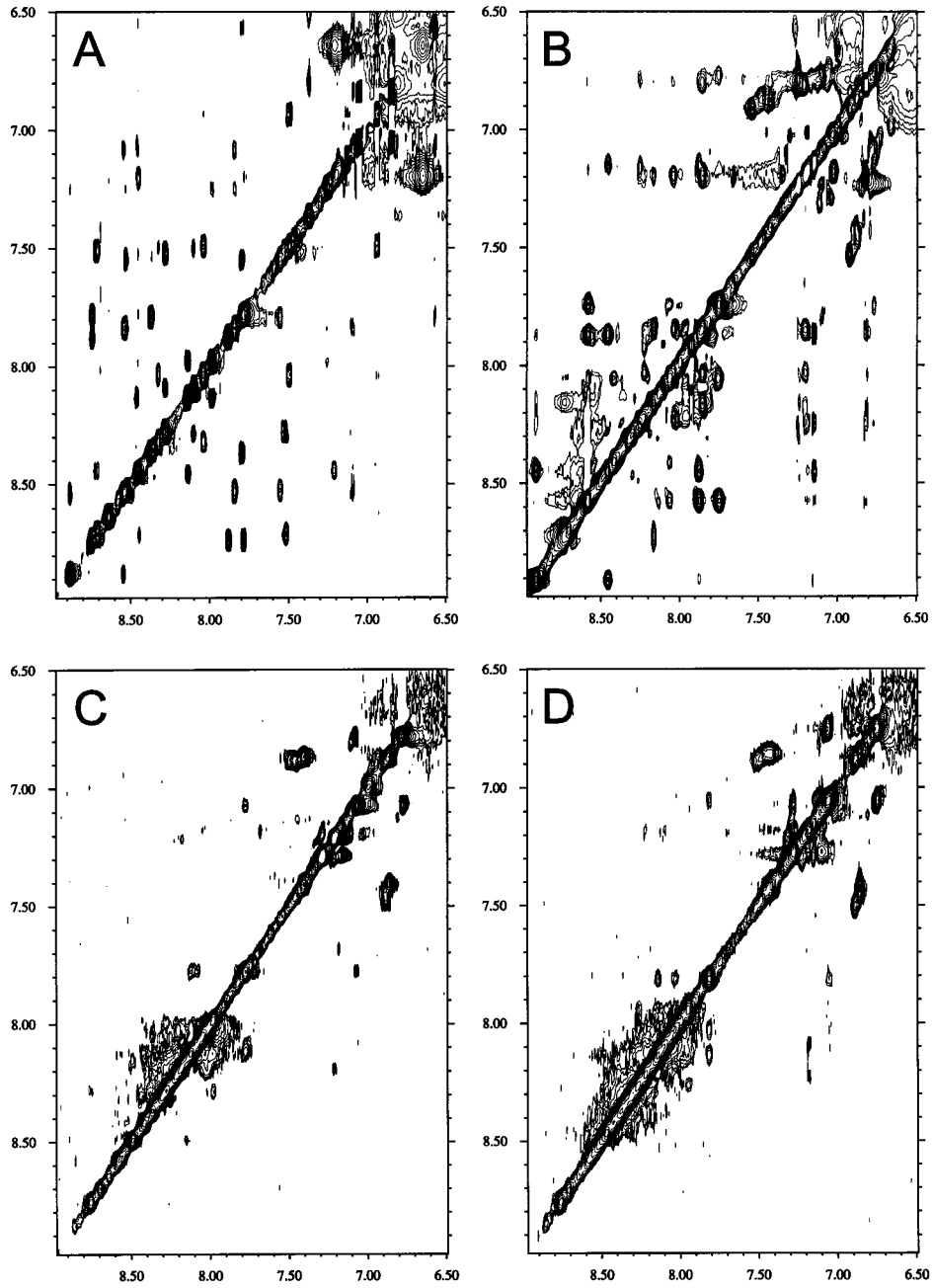

FIGURE 5: Plots of NN regions of 200 ms mixing time NOESY spectra (600 MHz) of (A) ShK (wild-type), (B) [Abu3,35]ShK$_{12-28,17-32}$, (C) [Abu12,28]ShK$_{3-35,17-32}$, and (D) [Abu 17,32]ShK$_{3-35,12,28}$ at 293 K. For consistency, spectra are displayed just above the noise level in each case.

the RMSD over the backbone atoms of residues 14−24 is 3.94 Å; over the first ShK helix (residues 14−19), it is 1.75 Å, and over the second (residues 21−24) it is 0.44 Å.

The critical residues for ShK binding to the potassium channel are Lys22 and Tyr23, with Arg11, Ser20, Arg24, and Phe27 playing lesser roles (*10*, *11*, *17*, *20*). In ShK, these residues form a contiguous surface, as illustrated in Figure 7B. In [Abu3,35]ShK$_{12-28,17-32}$, this binding surface is substantially altered, with the side chain of Arg11 much further from the Lys22−Tyr23 diad than in ShK (distance from Arg11 C^{ζ} to Lys22 N^{ζ} is 12.6 ± 2.4 Å in ShK compared with 20.4 ± 1.8 Å in the analogue, and from Arg11 C^{ζ} to the centroid of the Tyr23 aromatic ring 4.9 ± 0.2 Å in ShK compared with 23.2 ± 2.0 Å in the analogue). Superimposing the closest-to-average structures of ShK and the analogue over residues 11, 22, and 23 gives an RMSD of 5.47 Å over the C^{α} and C^{β} atoms, 4.74 Å over the backbone atoms N, C^{α}, and C, and 7.56 Å over all heavy atoms. Corresponding values for residues 22 and 23 are 0.15, 0.45, and 1.63 Å, and for residues 11 and 22, 2.43, 2.73, and 4.95 Å.

Truncated Analogues. The effect of truncating the polypeptide chain in addition to eliminating the Cys3−Cys35 disulfide bond was examined by NMR analysis of the truncated analogues [Nle21]ShK(9−32)$_{12-28,17-32}$ and [Cys(Acm)12,28, Nle21]ShK(9−32)$_{17-32}$. The synthesis of these analogues was described by Pennington et al. (*19*), who also found that the CD spectra of both did not resemble that of native toxin, and their activities were reduced to less than 0.1% of ShK (*19*). Consistent with these observations, ^{1}H NMR spectra of these analogues showed substantially reduced spectral dispersion compared with native ShK, their

Table 3: Structural Statistics for the 20 Energy-Minimized Structures of [Abu3,35]ShK$_{12-28,17-32}$ from X-PLOR[a]

RMS deviations from experimental distance restraints (Å) (328)[b]		0.029 ± 0.001
RMS deviations from experimental dihedral restraints (deg) (26)[b]		0.40 ± 0.12
RMS deviations from idealized geometry		
bonds (Å)		0.0117 ± 0.0005
angles (deg)		2.73 ± 0.04
impropers (deg)		0.39 ± 0.02
energies (kcal mol^{-1})		
E_{NOE}		13.5 ± 0.9
E_{cdih}		0.32 ± 0.21
E_{L-J}		−101 ± 6
$E_{bond} + E_{angle} + E_{improper}$		121 ± 4
E_{elec}		−392 ± 26
mean pairwise RMSD (Å)	backbone heavy atoms	all heavy atoms
residues 1−35	1.33 ± 0.47	2.30 ± 0.61
residues 4, 8−31, 34, 35[c]	0.73 ± 0.20	1.60 ± 0.35

[a] Selected as described in the Materials and Methods. Values represent mean ± SD. [b] The numbers of restraints are shown in parentheses. None of the structures had distance violations of >0.3 Å or dihedral angle violations of >5°. [c] Residues with $S_{\phi,\psi} > 0.8$.

chemical shifts being much closer to random coil values. Although essentially complete resonance assignments could be made for both analogues, a distinct lack of long- and medium-range connectivities confirmed their lack of native structure.

DISCUSSION

In this paper, we have described the synthesis, K^+ channel blocking activity, and conformation of analogues of ShK toxin lacking one of the three disulfide bonds. The analogues were produced by solid-phase methods using Fmoc/t-Bu chemistry. Exploitation of orthogonal Cys-protecting groups allowed the unambiguous placement of each disulfide bond without the possibility of disulfide scrambling (*40*−*42*). In this section, we consider the effects of disulfide deletion in ShK toxin on its K^+ channel blocking activity and, in the case of [Abu3,35]ShK$_{12-28,17-32}$, compare the effect on activity with the structural changes observed by NMR.

The response of ShK toxin to loss of its disulfide bridges is generally similar to that of other polypeptides and small proteins cross-linked by similar numbers of disulfides (summarized in ref *42*) in that one bridge, generally the most solvent-exposed, can be removed without complete loss of activity, whereas the loss of more buried bridges leads to more drastic reductions in structure and activity. All of the analogues with two disulfides deleted showed no measurable activity in the binding or functional assays, and therefore, their structures were not investigated by NMR. By contrast, the three analogues with only one disulfide deleted all displayed some activity, and it was of interest to determine how much native structure they retained. Initial inspection of their 1D ^{1}H spectra suggested that all three had undergone significant conformational changes, as reflected in the substantial loss of spectral dispersion (Figure 4). Analysis of 2D NOESY spectra indicated, however, that [Abu3,35]ShK$_{12-28,17-32}$ retained chemical shifts and medium-range NOEs characteristic of the native fold, and for this reason, we determined its solution structure.

The structures obtained showed that the two helical regions in [Abu3,35]ShK$_{12-28,17-32}$ were not as well formed as in the native toxin and that the N- and C-terminal regions of the analogue diverged significantly from the native structure now that they were no longer linked by a disulfide. These changes have major consequences for the relative disposition of the key functional groups for Kv1.3 channel binding, as shown in Figure 7. In particular, Arg11 has a markedly different orientation relative to Lys22 and Tyr23.

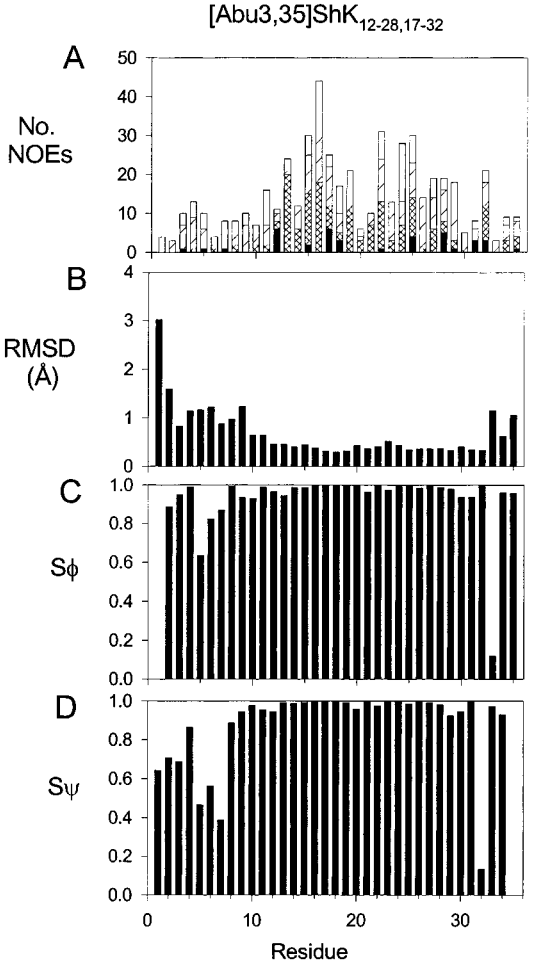

FIGURE 6: Parameters characterizing the final 20 structures of [Abu3,35]ShK$_{12-28,17-32}$, plotted as a function of residue number. (A) Upper-bound restraints used in final round of structural refinement shown as long-range (black), medium-range (cross-hatched), sequential (diagonal shading), and intraresidue (unshaded). (B) RMS differences from mean structure for N, C$^\alpha$, and C atoms following superposition over the whole molecule. (C and D) Angular order parameters (S) for the backbone dihedral angles ϕ and ψ.

These structural changes are larger than might have been expected given that the binding affinity of [Abu3,35]-ShK$_{12-28,17-32}$ for rat brain synaptosomes decreased by only 18-fold and for Kv1.3 channels by about 100-fold. In considering why the significant structural changes in [Abu3,35]ShK$_{12-28,17-32}$ have not caused a greater loss of activity, one possibility is that the solution structures change significantly upon K^+ channel binding, such that neither the native ShK solution structure nor that of [Abu3,35]-ShK$_{12-28,17-32}$ represents the bound structure. In this case, both polypeptides would have to undergo significant structural rearrangement upon binding, with the energy penalty being greater for [Abu3,35]ShK$_{12-28,17-32}$ than native toxin. While it is likely that there is some conformational change associated with channel binding, we do not believe it is

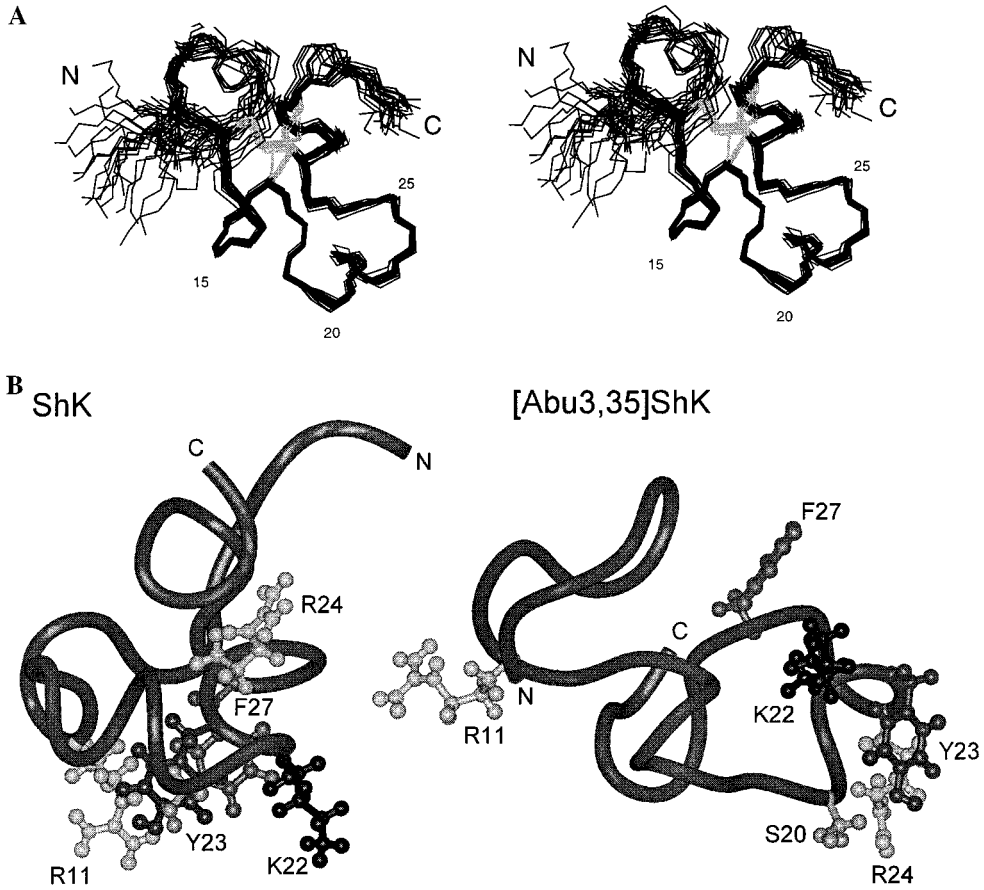

FIGURE 7: Solution structure of [Abu3,35]ShK$_{12-28,17-32}$. (A) Stereoview of the best 20 structures, superimposed over the backbone heavy atoms N, C$^{\alpha}$, and C of residues 8−31. Only the backbone heavy atoms are shown, except for the two disulfide bonds (Cys12−Cys28 and Cys17−Cys32) and the two Abu (3, 35) side chains, which are shown in a lighter shade. (B) Ribbon diagrams of the closest-to-average structures for [Abu3,35]ShK$_{12-28,17-32}$ (right) and ShK (left) superimposed over the backbone heavy atoms of residues 14−24 and shown in the same orientation. The side chains of key binding residues of ShK are shown in ball-and-stick representation in each molecule These residues represent a consensus from various studies of the K^+ channel binding surface of ShK (*10*, *11*, *17*, *20*); Lys9, which appeared to be important for lymphocyte binding (*10*), has not been confirmed by subsequent studies (*11*, *17*), and a role for His19 was inferred from an H19K mutant (*17*) and may, in any case, have a structural origin (*18*). This figure was generated using Insight II.

substantial. This is based on the fact that the solution structure of native ShK toxin can be docked with a model of the Kv1.3 channel based on the recent crystal structure of KcsA (*43*) in a way that accounts satisfactorily for the results of several complementary mutational analyses (*20*). Furthermore, an analogue of ShK toxin with additional stabilization in the first helix, and therefore less likely to undergo conformational changes, is nearly equipotent with ShK (our unpublished results).

Although the conformation of [Abu3,35]ShK$_{12-28,17-32}$ differs from that of native ShK, there is of course no barrier to its adopting a nativelike conformation as it contacts the vestibule of the potassium channel. The reduction in binding affinity might then reflect the energetic penalty associated with this 'induced fit'. Reduced binding affinities of 18- and 100-fold correspond to free-energy differences of 1.7 and 2.7 kcal/mol, respectively.

Another possible explanation for the good binding of [Abu3,35]ShK$_{12-28,17-32}$ follows from the 4-fold symmetry of the Kv1.3 channel. The analogue may bind in a nonnative conformation similar to that observed in solution, with Lys22 and Tyr23 making similar contacts with the pore and vestibule of the channel as native ShK, but Arg11 interacting with a different subunit. Of course, new interactions between the analogue and Kv1.3 may also contribute to its binding. At this stage, we cannot determine which of these possible explanations for the retention of binding affinity by [Abu3,35]ShK$_{12-28,17-32}$ is correct. An amalgam of induced fit to the receptor and some new interactions with the channel seems the most likely.

In the other two analogues, [Abu17,32]ShK$_{3-35,12-28}$ and [Abu12,28]ShK$_{3-35,17-32}$, more substantial losses of activity were evident, although they retained high nanomolar activity in the functional assays. The 2D NOESY spectra showed that their structures were even less nativelike than that of [Abu3,35]ShK$_{12-28,17-32}$, implying that their further loss of activity was due to an even greater loss of native structure. The fact that both of these full-length analogues retained some activity, however, indicates that the two remaining disulfide bridges in each case stabilize an overall topology which supports binding to the K^+ channel with less of an energetic penalty than in the case of the monocyclic analogues, where activity was not measurable. The residual activity of [Abu17,32]ShK$_{3-35,12-28}$ and [Abu12,28]-ShK$_{3-35,17-32}$ thus highlights a distinction between the loss of native secondary and tertiary structure on one hand and the retention of global topology imposed by native disulfide bridges on the other.

The observation that even the least active dicyclic analogue retained measurable activity may also reflect the fact that

many of the key residues for channel binding are clustered in the amino acid sequence. Some structural stabilization of this cluster of residues is clearly necessary, as evidenced by the lack of activity of the monocyclic analogues. Nevertheless, these results bode well for future attempts to reproduce the favorable biological activity of ShK toxin in a low molecular weight mimic, either peptidic or nonpeptidic.

ACKNOWLEDGMENT

We thank Luette Forrest and Annabelle Chailing Wu for excellent technical assistance.

SUPPORTING INFORMATION AVAILABLE

Three tables of chemical shifts (for [Abu3,35]$ShK_{12-28,17-32}$ and the two truncated analogues) and three figures (a summary of NOEs and coupling constants for [Abu3,35]-$ShK_{12-28,17-32}$ and two figures of chemical shift comparisons). This material is available free of charge via the Internet at http://pubs.acs.org.

REFERENCES

1. Miller, C. (1995) *Neuron 15*, 5−10.
2. Harvey, A. L., and Anderson, A. J. (1985) *Pharmacol. Ther. 31*, 33−55.
3. Terlau, H., Shon, K. J., Grilley, M., Stocker, M., Stuhmer, W., and Olivera, B. M. (1996) *Nature 381*, 148−151.
4. Castañeda, O., Sotolongo, V., Amor, A. M., Stöcklin, R., Anderson, A. J., Harvey, A. L., Engström, Å, Wernstedt, C., and Karlsson, E. (1995) *Toxicon 33*, 603−613.
5. Cotton, J., Crest, M., Bouet, F., Alessandri, N., Gola, M., Forest, E., Karlsson, E., Castañeda, O., Harvey, A. L., Vita, C., and Menez, A. (1997) *Eur. J. Biochem. 244*, 192−202.
6. Pennington, M. W., Byrnes, M. E., Zaydenberg, I., Khaytin, I., de Chastonay, J., Krafte, D., Hill, R., Mahnir, V., Volberg, W. A., Gorczyca, W., and Kem, W. R. (1995) *Int. J. Pept. Protein Res. 46*, 354−358.
7. Pohl, J., Hubalek, F., Byrnes, M. E., Nielsen, K. R., Woods, A., and Pennington, M. W. (1995) *Lett. Pept. Sci. 1*, 291−297.
8. Tudor, J. E., Pallaghy, P. K., Pennington, M. W., and Norton, R. S. (1996) *Nat. Struct. Biol. 3*, 317−320.
9. Bontems, F., Gilquin, B., Roumestand, C., Menez, A., and Toma, F. (1992) *Biochemistry 31*, 7756−7764.
10. Pennington, M. W., Mahnir, V. M., Krafte, D. S., Zaydenberg, I., Byrnes, M. E., Khaytin, I., Crowley, K., and Kem, W. R. (1996) *Biochem. Biophys. Res. Commun. 219*, 696−701.
11. Pennington, M. W., Mahnir, V. M., Khaytin, I., Zaydenberg, I., Byrnes, M. E., and Kem, W. R. (1996) *Biochemistry 35*, 16407−16411.
12. Pennington, M. W., Karlsson, E., and Kem, W. R. (1997) in *Guidebook to Protein Toxins and Their Use in Cell Biology* (Montecucco, C., and Rappuoli, R., Eds.) pp 159−161, Oxford University Press.
13. Dauplais, M., Leqoc, A., Song, J. X., Cotton, J., Jamin, N., Gilquin, B., Roumestand, C., Vita, C., de Medeiros, C. L. C., Rowan, E. G., Harvey, A. L., and Menez, A. (1997) *J. Biol. Chem. 272*, 4302−4309.
14. Stampe, P., Kolmakova-Partensky, L., and Miller, C. (1994) *Biochemistry 33*, 443−450.
15. Hidalgo, P., and MacKinnon, R. (1995) *Science 268*, 307−310.
16. Aiyar, J., Withka, J. M., Rizzi, J. P., Singleton, D. H., Andrews, G. C., Lin, W., Boyd, J., Hanson, D., Simon, M., Dethlefs, B., Lee, C.-L., Hall, J. E., Gutman, G. A., and Chandy, K. G. (1995) *Neuron 15*, 1169−1181.
17. Rauer, H., Pennington, M. W., Cahalan, M. D., and Chandy, K. G. (1999) *J. Biol. Chem. 274*, 21885−21892.
18. Tudor, J. E., Pennington, M. W., and Norton, R. S. (1998) *Eur. J. Biochem. 251*, 133−141.
19. Pennington, M. W., Mahnir, V. M., Baur, P., McVaugh, C. T., Behm, D., and Kem, W. R. (1997) *Protein Pept. Lett. 4*, 237−242.
20. Kalman, K., Pennington, M. W., Lanigan, M. D., Nguyen, A. Rauer, H., Mahnir, V., Paschetto, K., Kem, W. R., Grissmer, S., Gutman, G. A., Christian, E. P., Cahalan, M. D., Norton, R. S., and Chandy, K. G. (1998) *J. Biol. Chem. 273*, 32697−32707.
21. King, D. S., Fields, C. G., and Fields, G. B. (1990) *Int. J. Pept. Protein Res. 36*, 255−266.
22. Ellman, G. L. (1959) *Arch. Biochem. Biophys. 82*, 70−77.
23. Veber, D. F., Milkowski, J. D., Varga, S. L., Denkewalter, R. G., and Hirschmann, R. (1972) *J. Am Chem. Soc. 94*, 5456−5461.
24. Kem, W. R., Sanyals, G., Williams, W. R., and Pennington, M. W. (1996) *Lett. Pept. Sci. 3*, 69−72.
25. Pallaghy, P. K., Alewood, D., Alewood, P. F., and Norton, R. S. (1997) *FEBS Lett. 419*, 191−196.
26. Sklenar, V., Piotto, M., Leppik, R., and Saudek, V. (1993) *J. Magn. Reson., Ser. A 102*, 241−245.
27. Güntert, P., Mumenthaler, C., and Wüthrich, K. (1997) *J. Mol. Biol. 273*, 283−298.
28. Brünger, A. T. (1992) *X-PLOR Version 3.1. A System for X-ray Crystallography and NMR*, Yale University, New Haven, CT.
29. Bernstein, F. C., Koetzle, T. F., Williams, G. J., Meyer, E. E. Jr., Brice, M. D., Rodgers, J. R., Kennard, O, Shimanouchi, T., and Tasumi, M. (1977) *J. Mol. Biol. 112*, 535−542.
30. Laskowski, R. A., Rullmann, J. A. C., MacArthur, M. W., Kaptein, R., and Thornton, J. M. (1996) *J. Biomol. NMR 8*, 477−486.
31. Koradi, R., Billeter, M., and Wüthrich, K. (1996) *J. Mol. Graphics 14*, 51−55.
32. Grissmer, S., Nguyen, A. N., Aiyar, J., Hanson, D. C., Mather, R. J., Gutman, G. A., Karmilowicz, M. J., Auperin, D. D., and Chandy, K. G. (1994) *Mol. Pharmacol. 45*, 1227−1234.
33. Fanger, C. M., Ghanshani, S., Logsdon, N. J., Rauer, H., Kalman, K., Zhou, J., Beckingham, K., Chandy, K. G., Cahalan, M. D., and Aiyar J. (1999) *J Biol. Chem. 274*, 5746−5754.
34. Rauer, H., and Grissmer, S. (1996) *Mol. Pharm. 50*, 1625−1634.
35. Vasquez, J. J., Feigenbaum, P., King, V. F., Kaczorowski, G. J., and Garcia, M. L. (1990) *J. Biol. Chem. 265*, 15564−15571.
36. Fujiwara, Y., Akaji, K., and Kiso, Y. (1994) *Chem. Pharm. Bull. 42*, 724−726.
37. Shamotienko, O. G., Parcej, D. N., and Dolly, J. O. (1997) *Biochemistry 36*, 8195−8201.
38. Koschak, A., Bugianesi, R. M., Mitterdorfer, J., Kaczorowski, G. J., Garcia, M. L., and Knaus, H. G. (1998) *J. Biol. Chem. 273*, 2639−2644.
39. Wishart, D. S., Bigam, C. G., Holm, A., Hodges, R. S., and Sykes, B. D. (1995) *J. Biomol. NMR 5*, 67−81.
40. Andreu, D., Albericio, F., Sole, N. A., Munson, M. C., Ferrer, M. and Barany, G. (1994) in *Methods in Molecular Biology Vol. 35: Peptide Synthesis Protocols* (Pennington, M. W., and Dunn, B. M., Eds.) pp 91−169, Humana Press, Totowa, NJ.
41. Moroder, L., Besse, D., Musiol, H. J., Rudolphbohner, S., and Siedler, F. (1996) *Biopolymers 40*, 207−234.
42. Flinn, J. P., Pallaghy, P. K., Lew, M. J., Murphy, R., Angus, J. A., and Norton, R. S. (1999) *Biochim. Biophys. Acta* (in press).
43. Doyle, D. A., Cabral, J. M., Pfuetzner, R. A., Kuo, A., Gulbis, J. M., Cohen, S. L., Chait, B. T., and MacKinnon, R. (1998) *Science 280*, 69−77.

BI991282M